DOI: 10.1002/ejic.201000201

NIR Bioimaging: Development of Liposome-Encapsulated, Rare-Earth-Doped Y_2O_3 Nanoparticles as Fluorescent Probes

Kohei Soga,*[a,b,c] Kimikazu Tokuzen,[a] Kosuke Tsuji,[a] Tomoyoshi Yamano,[d] Hiroshi Hyodo,[a,b,c] and Hidehiro Kishimoto[c,d]

Keywords: Bioimaging / Rare earths / Liposomes / Ceramics / Fluorescent probes / Nanoparticles

Near-infrared (NIR) bioimaging is attracting a lot of attention due to the absence of strong scattering and color fading of the phosphors, which can provide long-term and deep imaging. For fluorescence bioimaging (FBI) in the NIR region, rare-earth-doped ceramic nanoparticles can be one of the best candidates. For the delivery of the ceramic particles to the biological imaging target, liposome-encapsulating the ceramic phosphor is proposed. Liposome-encapsulated, Er-doped Y_2O_3 nanoparticles were prepared as fluorescent probes for NIR bioimaging. Their surface was modified with PEG, biotin, anionic, and cationic agents. The dispersion, surface charge, and specific interactions of the surface-modified liposomes were characterized. Microscopic and macroscopic NIR bioimages were demonstrated by injecting the liposome-encapsulated, Er-doped Y_2O_3 nanoparticles into the body of a mouse through the blood vessels. The NIR fluorescence images of the mouse organs are presented.

Introduction

Fluorescence bioimaging (FBI) is one of the most important methods for biological research and medical diagnosis to visualize the spatial distribution and transient movement of substances in biological systems as multicolor images. Currently, major problems of FBI are shallow observation depth due to scattering, color fading of the organic phosphors, autofluorescence that causes background noise, and damage to the biological objects, which are mostly caused by the irradiation of short-wavelength excitation light, such as UV or blue light, to obtain visible fluorescence.[1] On the other hand, the fluorescence may not be "visible" to the naked eye, as most bioimaging procedures are carried out by using charge-coupled device (CCD) cameras. Therefore, the FBI in the near-infrared (NIR) is attracting interests in the fields of biological and medical research. The NIR wavelength region between 800 and 1700 nm is known as a "biological window" where one can expect the lowest loss of light due to scattering.[2] The region does not suffer from IR absorption due to molecular vibration. Because of the low quantum energy of the photon in this region, the light to be used for excitation is not harmful to biological subjects and fluorescent phosphors.

As materials that can emit fluorescence in the NIR region, rare-earth-doped ceramics have been applied as laser or optical amplifier media for decades. 1064 nm emission under 800 nm excitation from Nd:YAG is used for one of the most popular solid-state lasers.[3] 1550 nm emission under 980 nm excitation from Er^{3+}-doped silicate glass fiber is used for optical amplifiers in optical communication.[4] Those applications originate from the characteristic electronic states of 4f electrons, narrow-energy bands, and weak electron–phonon coupling, as results of the shielding effect by the outer-lying filled 5s and 5p shells. Some of the rare-earth-doped ceramics are known to show upconversion (UC) emission, which is an infrared-to-visible conversion through stepwise excitation among the discrete energy levels of the rare-earth ions in ceramics.[1] The use of this phenomenon for bioimaging has been proposed since 1999.[5–11] Our group has also worked on UC FBI in the recent years, focusing on the development of imaging probe materials.[1,12–18]

In recent years, we have been developing NIR-NIR bioimaging systems by using the NIR fluorescence at 1550 nm under 980 nm excitation, which can be efficiently emitted from Er-doped yttrium oxide (Y_2O_3:Er^{3+}) phosphors, as shown in Figure 1.[19] The development of the imaging system now allows the application of InGaAs-CCD, which can detect the light in the NIR wavelength region.

[a] Department of Materials Science and Technology, Tokyo University of Science,
2641 Yamazaki, Noda, Chiba 278-8510, Japan
Fax: +81-4-7124-1526
E-mail: mail@ksoga.com
[b] Polyscale Technology Research Center (PTRC), Tokyo University of Science,
2641 Yamazaki, Noda, Chiba 278-8510, Japan
[c] Center for Technologies against Cancer (CTC), Tokyo University of Science,
2669 Yamazaki, 278-0022 Chiba, Japan
[d] Research Institute for Biological Sciences, Tokyo University of Science,
2669 Yamazaki, 278-0022 Chiba, Japan

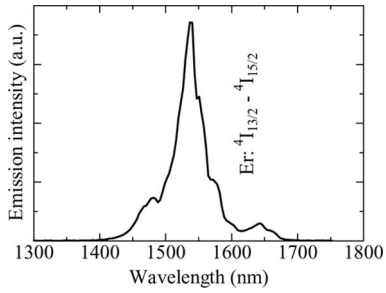

Figure 1. Emission spectrum of Er-doped Y_2O_3 nanoparticles in the NIR region.[19]

To use the Y_2O_3:Er^{3+} nanoparticles for NIR bioimaging, it is required to deliver the particles to the targeted part of the biological system. Liposome is a good candidate as a material with a similar structure as the cell membrane, and the use of liposome has been attracting interest in the research field of drug delivery. In the present study, liposome-encapsulated Y_2O_3:Er^{3+} nanoparticles with various surface properties were prepared. The obtained liposomes were tested by using an NIR fluorescence plate assay. As a demonstration of NIR-NIR bioimaging, the distribution of the liposomes injected through the blood vessels into the body of a mouse was also observed by using microscopic and macroscopic NIR FBI systems.

Results and Discussion

The encapsulation of the Y_2O_3:Er^{3+} nanoparticles were checked by observation by FE-SEM. Figure 2 shows the FE-SEM images of the liposome encapsulation of the particles under different accelerating voltages. Figure 2(a) shows the image under smaller voltage, where the outlines of the liposomes were observed. In Figure 2(b), under higher voltage, the Y_2O_3:Er^{3+} nanoparticles were observed through the liposome skin layer. From those images, we conclude that the Y_2O_3:Er^{3+} nanoparticles were encapsulated in the liposome. The average size of the Y_2O_3:Er^{3+} nanoparticles were approximately 150 nm, which matches the size estimated by dynamic light scattering (DLS) before the encapsulation. We have previously reported that particle size estimations by SEM, TEM, and DLS match.[17] The size of the liposomes dried in vacuo and observed under a microscope were approximately 500 nm.

Figure 3 shows the fluorescence images of the liposome-encapsulated Y_2O_3:Er^{3+} nanoparticles under an optical microscope. The bright-field image [Figure 3(a)] shows that the size of the wet liposome is approximately 650 nm. Figure 3(b, c) shows the upconversion fluorescence image,[1] which can be observed with a CCD camera for visible light under 980 nm NIR excitation. Figure 3(d) shows the NIR fluorescence image at 1550 nm, which was observed by an NIR CCD camera. The difference between the scales of a–c and d is due to the difference in the resolution of the used CCD cameras. All of the pictures show that the liposome is filled with Y_2O_3:Er^{3+} nanoparticles.

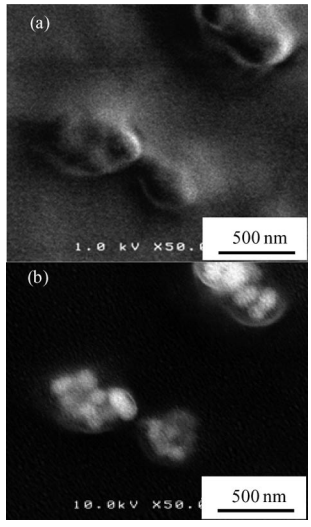

Figure 2. FE-SEM images of liposome-encapsulated Y_2O_3:Er^{3+} nanoparticles. Accelerating voltages are (a) 1 kV and (b) 10 kV.

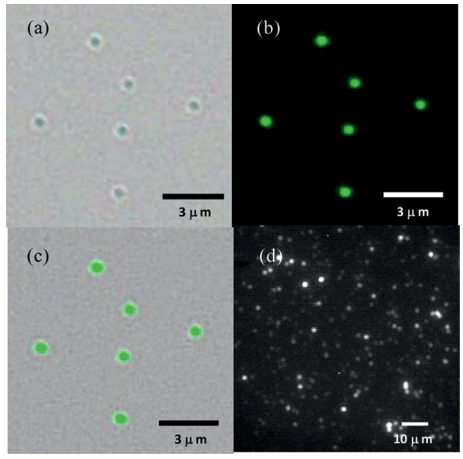

Figure 3. Fluorescence microscope images of liposome-encapsulated Y_2O_3:Er^{3+} nanoparticles. Imaging schemes are (a) bright-field image, (b) UC fluorescence image, (c) (a) + (b) and (d) NIR fluorescence image.

Because of the use of dipalmitoyl phosphatidylglycerol (DPPG), the surface of the liposome should be negatively charged. Figure 4 shows the ζ potentials of the bare and liposome-encapsulated Y_2O_3 particles. It is known that Y_2O_3 is positively charged under neutral conditions,[15] as shown in the figure. In contrast to semiconductor or metal particles, ceramic nanoparticles are normally insulators, and their surface charge cannot be determined by the type of electric carrier. Y_2O_3 comprises ionic bonding. The positive charge may be caused by the higher positive charge of Y^{3+} relative to that of O^{2-}, which causes higher localized positive charge. On the other hand, the liposome-encapsulated Y_2O_3 shows strong negative charge, which implies that the surface of the liposome consists of negatively charged DPPG.

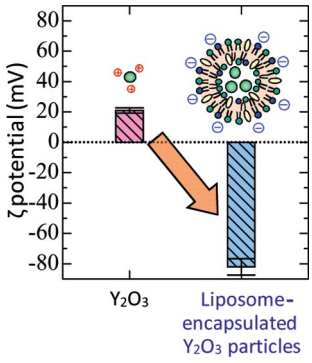

Figure 4. ζ potential of Y_2O_3 particles and liposome-encapsulated Y_2O_3 particles at pH 7.0.

Ceramic nanoparticles are normally dispersed in pure water because of the surface charge of the ceramics. However, under physiological conditions with strong ionic character, the charge is cancelled, and they agglomerate quickly to decrease the large specific energy. Figure 5 shows the transient change in the transmittance of the suspension of the bare and liposome-encapsulated Y_2O_3 nanoparticles measured at 550 nm. In case of the bare Y_2O_3 nanoparticles, the transmittance quickly decreases because of the sedimentation of the particles due to agglomeration. On the other hand, in the case of the liposome-encapsulated particles, it slowly decreases. The encapsulation of the particles by the liposome is shown to enhance the dispersion stability of the Y_2O_3 nanoparticles as bioimaging fluorescence probes.

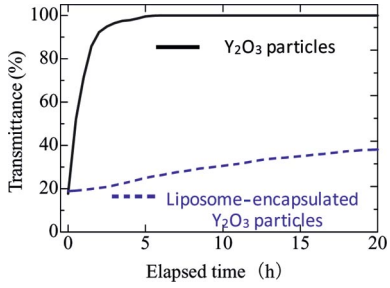

Figure 5. Sedimentation behavior of bare and liposome-encapsulated Y_2O_3 particles in a physiological saline solution (150 mM $NaCl_{aq}$, with pH 7.0).

Important characteristics of fluorescent probes to be used as bioimaging probes are dispersion stability under physiological conditions, the absence of nonspecific interaction with nontargeted substances, and specific interaction with the targeted objects. The first requirement is present in the liposome-encapsulated Y_2O_3 nanoparticles, as shown in Figure 5. Specific interaction with the targeting object was achieved by introducing PEG and biotin in the liposome skin layer. PEG is known to avoid nonspecific interaction with subjects for the use of materials with biological functions.[13–15,20–33] Biotin is a molecule known to specifically interact only with avidin in the biological system. By using streptavidin, biotinylated agents can be specifically combined to other biotinylated ligands to deliver the agents to a target. In this work, PEG and biotin were introduced to the surface of the liposome by using PEG-distearoylglycerol (PEG-DSG) and dipalmitoyl phosphoethanolamine-*N*-biotinylsodium salt (DPPE-biotin). Upon the introduction of the PEG-DSG and/or DPPE-biotin, there was no obvious change in the SEM and optical microscope observation. Figure 6 shows the results of the fluorescence plate assay by the fluorescence of the Y_2O_3:Er^{3+} nanoparticles at 1550 nm under 980 nm excitation. The tested plates are with streptavidin as a target agent and bovine serum albumin (BSA) as a nontarget protein.

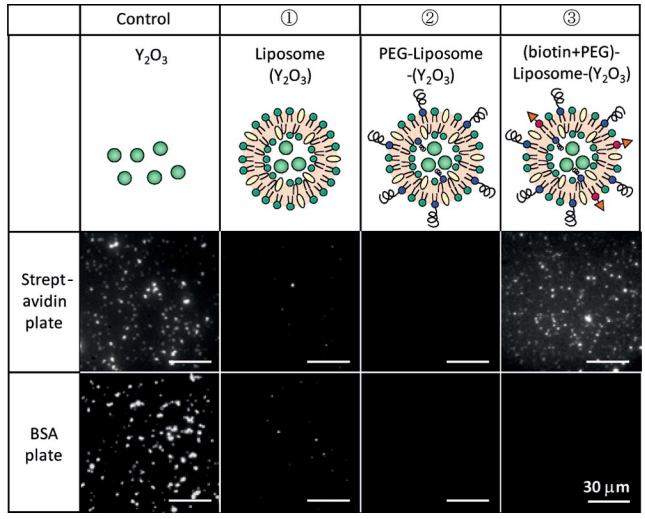

Figure 6. Evaluation of specific interaction of liposome-encapsulated Y_2O_3:Er^{3+} nanoparticles by fluorescence plate assay on streptavidin and BSA plates. Bare and liposome-encapsulated Y_2O_3:Er^{3+} nanoparticles are compared to those in which the liposome was modified with PEG and with PEG and biotin.

The bare Y_2O_3:Er^{3+} nanoparticles interacted with both plates. The Y_2O_3:Er^{3+} particles encapsulated in the liposome interacted much less than the bare particles, though still some particles were observed on both plates. The Y_2O_3:Er^{3+} nanoparticles encapsulated in PEGylated liposomes were not observed in any of the plates. This result shows that the PEGylation certainly avoids the nonspecific interaction of the liposome-encapsulated Y_2O_3:Er^{3+} nanoparticles with proteins. By introducing biotin into the PEGylated liposome, the Y_2O_3:Er^{3+} nanoparticles can only be observed on the surface of the streptavidin plate and not on the BSA plate. As a result, liposome-encapsulated Y_2O_3:Er^{3+} nanoparticles with both PEGylation and biotin modification are useful as a probe for NIR biological imaging.

As a demonstration of the use of the liposome-encapsulated Y_2O_3:Er^{3+} nanoparticles as bioimaging probes, the liposomes were injected into a mouse and its organs were observed by using macroscopic and microscopic NIR FBI systems. The surfaces of the liposomes were controlled to be anionic, cationic, and PEGylated by using DPPG, stearylamine, and PEG-DSG, respectively. Figure 7 shows the NIR fluorescence images at 1550 nm under 980 nm excitation. The injected suspension was HEPES buffer (2 mL,

20 mM) with NaCl (150 mM) dispersed with Y_2O_3:Er^{3+} particles (5 mg/mL). For the following cases, a certain amount of Yb^{3+} was co-doped into Y_2O_3:Er^{3+} as a fluorescence sensitizer. The mouse skin was opened for clear observation. In all cases, the fluorescence of the Y_2O_3:Er^{3+} nanoparticles was observed from the liver. The results show that the lipofected Y_2O_3:Er^{3+} nanoparticles tend to concentrate in the liver when injected into the blood vessel via the tail vain.

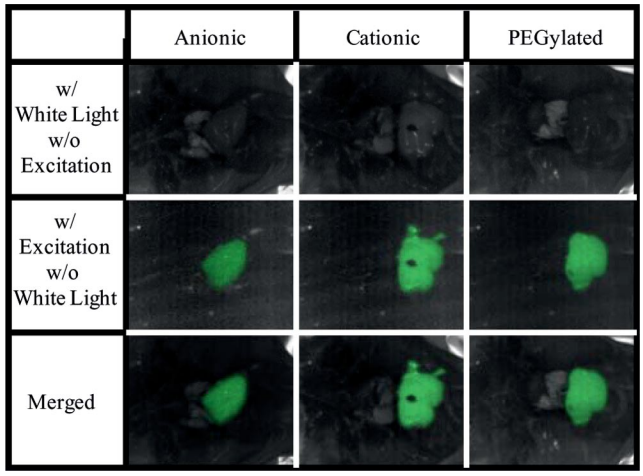

Figure 7. NIR fluorescence images of mouse organs injected with anionic, cationic, and PEGylated liposome-encapsulated Y_2O_3:Er^{3+} nanoparticles. The brightly illuminated organ is the liver.

Figure 8 shows the NIR fluorescence microscopic images of the sections from various organs of the same mouse as above. Certain amounts of the particles were found in both the liver and the spleen. No particles were found in the kidney. The difference due to the PEGylation was found in the spleen. Liposome particles with anionic and cationic surface were found both in the liver and in the spleen, while those with PEGylation were not found in the spleen. Studies to clarify the biological and medical meaning of this distribution of the probes are now in progress.

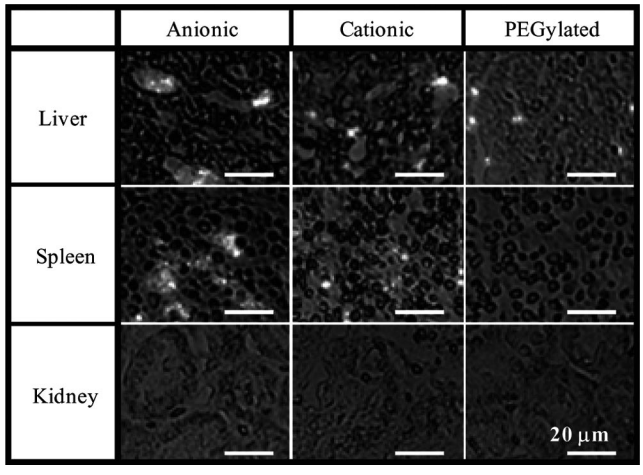

Figure 8. NIR fluorescence microscopic images of histological sections of various organs of a mouse injected with anionic, cationic, and PEGylated liposome-encapsulated Y_2O_3:Er^{3+} nanoparticles.

Conclusions

Liposome-encapsulated, Er-doped Y_2O_3 nanoparticles with various surface modifications as a fluorescent probe for NIR bioimaging were successfully fabricated. By introducing PEG on the surface of the liposome, nonspecific interaction with a protein was avoided. The liposome whose surface was modified with both biotin and PEG specifically interacted with streptavidin. Organs of a mouse injected with the liposome were imaged by both microscopic and macroscopic NIR imaging systems as a demonstration of NIR bioimaging.

Experimental Section

The preparation of Y_2O_3:Er^{3+} nanoparticles is described precisely elsewhere.[13–17] The particles were obtained by calcination of the precursor precipitated by using homogeneous precipitation. The obtained particles can emit 550 and 660 nm visible light through the upconversion process and 1550 nm light through the normal fluorescence process under 980 nm excitation by a laser diode.

Liposome-encapsulated Y_2O_3:Er^{3+} nanoparticles were prepared by the complex emulsion method.[34] HEPES buffer (2 mL, 10 mmol/L, pH 7.4 with 150 mmol/L NaCl) dispersed with PEG-modified Y_2O_3:Er^{3+} particles[14] (5 mg/mL) was added to phospholipid solution (4 mL) to form a water-in-oil (W/O) emulsion. The phospholipid solution was a chloroform solution with dipalmitoyl phosphatidylcholine (DPPC), DPPG, and cholesterol. The concentration was adjusted so that the total lipid concentration would be 30 μmol/L. The W/O emulsion was then moved to HEPES buffer solution (200 mL, 20 mmol/L, pH 7.4 with 150 mmol/L NaCl) with DPPC to form a water-in-oil-in-water (W/O/W) emulsion. The solution was stirred during the mixing and after the mixing for 12 h in a fume hood to evaporate the chloroform at room temperature. The absence of cloroform was checked by smelling the solution. DS-PEG and DPPE-biotin were added to the buffer solution at the last stage for the introduction of the PEG and biotin. The obtained liposome-encapsulated Y_2O_3:Er^{3+} nanoparticles were centrifugally washed two times with HEPES buffer solution (200 mL, 20 mmol/L, pH 7.4 with 150 mmol/L NaCl). The liposome-encapsulated Y_2O_3:Er^{3+} nanoparticles were finally dispersed in the same buffer solution such that the Y_2O_3:Er^{3+} concentration was 5 mg/mL.

The liposome solutions injected to the mouse were prepared by the method described above with the compositions listed in Table 1.

Table 1. Percent composition of the solution of the liposome injected to the mouse [mol-%].

Liposome	DPPC	Cholesterol	Additive	Amount
Anionic	40	40	DPPG	20
Cationic	40	40	stearylamine	20
PEGylated	50	40	PEG-DSG	10

The samples were injected into the blood vessel of a mouse via the tail vain. The mouse was kept alive in a cage for two hours and moved for organ imaging. The mouse was sacrificed for histology 20 min after the organ imaging. For the histological observation, the organs of the mouse were dissected, embedded in Tissue-Tek (Sacura), and snap frozen in liquid nitrogen. 7 μm cryosections were fixed in acetone at –20 °C and air-dried for 30 min. The section was stained with hematoxylin–eosin (HE) and subjected to the microscopic observation shown in Figure 8.

The NIR microscopic bioimaging system is equipped with a NIR CCD (InGaAs-CCD), as well as a laser diode at 980 nm. The optical components, such as the lens, mirror, and filters are designed so that one can observe an image with 1550 nm emission under 980 nm excitation.

The NIR macroscopic bioimaging system, so-called in vivo imaging system (IVIS), consists of a 980 nm fiber-pigtailed diode laser, a laser scanner, and a NIR (InGaAs) CCD camera, which can capture images in the 800–1700 nm wavelength region.

Acknowledgments

The authors thank to Prof. Y. Nagasaki of the University of Tsukuba and his group member for advisories on experiments. This work was supported by "Academic Frontier" Project for Private Universities: Matching Fund Subsidy from MEXT (Ministry of Education, Culture, Sports, Science and Technology), 2006-2010/ 2009-2013.

[1] K. Soga, *Application of Ceramic Nanophosphors for Biomedical Photonics* (Ed.: M. C. Tan), Transworld Research Network, Kerala, India, **2009**, pp. 223–241.
[2] R. R. Anderson, J. A. Parrash, *J. Invest. Dermatol.* **1981**, *77*, 13–19.
[3] R. C. Powell, *Physics of Solid State Laser Materials*, Springer, New York, NY, **1998**.
[4] S. Sudo (Ed.), *Optical Fiber Amplifiers: Materials, Devices, and Applications*, Artech House Publishers, Norwood, MA, **1997**.
[5] H. J. M. A. A. Jijlmans, J. Bonnet, J. Burton, K. Kardos, T. Vail, R. S. Niebala, H. J. Tanke, *Anal. Biochem.* **1999**, *267*, 30–36.
[6] P. Corstjens, M. Zuiderwijk, A. Brink, S. Li, H. Feindt, R. S. Neidbala, H. Tanke, *Clin. Chem.* **2001**, *47*, 1885.
[7] F. van de Rijke, H. Zijlmans, S. Li, T. Vail, A. K. Raap, R. S. Niedbala, H. J. Tanke, *Nat. Biotechnol.* **2001**, *19*, 273–276.
[8] J. Hampl, M. Hall, N. A. Mufti, Y. M. M. Yao, D. B. MacQueen, W. H. Wright, D. E. Cooper, *Anal. Biochem.* **2001**, *288*, 176–187.
[9] R. S. Niedbala, H. Feindt, K. Kardos, T. Vail, J. Burton, B. Bielska, S. Li, D. Milunic, P. Bourdelle, R. Vallejo, *Anal. Biochem.* **2001**, *293*, 22–30.
[10] K. Kuningas, T. Ukonaho, H. Pakkila, T. Rantanen, J. Rosenberg, T. Lovgren, T. Soukka, *Anal. Chem.* **2006**,*76*, 4690–4696.
[11] C. G. Morgan, A. C. Mitchell, *Biosens. Bioelectron.* **2007**, *22*, 1769–1775.
[12] K. Soga, T. Tsuji, F. Tashiro, J. Chiba, M. Oishi, K. Yoshimoto, Y. Nagasaki, K. Kitano, S. Hamaguchi, *J. Phys., Conf. Ser.* **2008**, *106*, 012023–1–5.
[13] Y. Saito, K. Shimizu, M. Kamimura, H. Furusho, K. Soga, Y. Nagasaki, *Trans. Mater. Res. Soc. Jpn.* **2008**, *33*, 803–806.
[14] K. Soga, R. Koizumi, M. Yamada, D. Matsuura, Y. Nagasaki, *J. Photopolym. Sci. Technol.* **2005**, *18*, 73–74.
[15] M. Kamimura, D. Miyamoto, Y. Saito, K. Soga, Y. Nagasaki, *Langmuir* **2008**, *24*, 8864–8870.
[16] T. Zako, H. Nagata, N. Terada, M. Sakono, K. Soga, M. Maeda, *J. Mater. Sci.* **2008**, *45*, 5325–5330.
[17] N. Venkatachalam, Y. Saito, K. Soga, *J. Am. Ceram. Soc.* **2009**, *92*, 1006–1010.
[18] T. Zako, H. Nagata, N. Terada, A. Utsumi, M. Sakono, M. Yohda, H. Ueda, K. Soga, M. Maeda, *Biochem. Biophys. Res. Commun.* **2009**, *381*, 54–58.
[19] K. Soga, K. Tokuzen, K. Tsuji, T. Yamano, N. Venkatachalam, H. Hyodo, H. Kishimoto, *Proc. SPIE* **2010**, *7598*, 759807 (9 pp.).
[20] S. Sivakumar, P. R. Diamente, F. C. van Veggel, *Chem. Eur. J.* **2006**, *12*, 5878–5884.
[21] P. R. Diamente, R. D. Burke, F. C. J. M. van Veggel, *Langmuir* **2006**, *22*, 1782–1788.
[22] P. R. Diamente, F. C. J. M. van Veggel, *J. Fluoresc.* **2005**, *15*, 543–551.
[23] S. F. Lim, R. Riehn, W. S. Ryu, N. Khanarian, C. K. Tung, D. Tank, R. H. Austin, *Nano Lett.* **2006**, *6*, 169–174.
[24] C. Woghiren, B. Sharma, S. Stein, *Bioconjugate Chem.* **1993**, *4*, 314–318.
[25] H. F. Gaertner, R. E. Offord, *Bioconjugate Chem.* **1996**, *47*, 38–44.
[26] Y. Akiyama, H. Otsuka, Y. Nagasaki, M. Kato, K. Kataoka, *Bioconjugate Chem.* **2000**, *11*, 947–950.
[27] S. Zhang, J. Du, R. Sun, X. Li, D. Yang, S. Zhang, C. Xiong, Y. Peng, *React. Funct. Polym.* **2003**, *56*, 17–25.
[28] F. M. Veronese, *Biomaterials* **2001**, *22*, 405–417.
[29] M. J. Roberts, M. D. Bentley, J. M. Harris, *Adv. Drug Delivery Rev.* **2002**, *54*, 459–476.
[30] H. Otsuka, Y. Nagasaki, K. Kataoka, *Adv. Drug Delivery Rev.* **2003**, *5*, 403–419.
[31] P. Caliceti, M. Chinol, M. Roldo, F. M. Veronese, A. Semenzato, S. Salmaso, G. Paganelli, *J. Controlled Release* **2002**, *83*, 97–108.
[32] R. B. Greenwald, Y. H. Choe, J. McGuire, C. D. Conover, *Adv. Drug Delivery Rev.* **2003**, *55*, 217–250.
[33] T. Ishii, H. Otsuka, K. Kataoka, Y. Nagasaki, *Langmuir* **2004**, *20*, 561–564.
[34] F. Ishii, A. Takamura, H. Ogata, *J. Dispersion Sci. Technol.* **1988**, *9*, 1–15.

Received: February 19, 2010
Published Online: May 14, 2010

